Study of Bi-Directional Buck-Boost Converter Topologies for Application in Electrical Vehicle Motor Drives

F. Caricchi (*), F. Crescimbini (*), F. Giulii Capponi (*), L. Solero (**)

(*) University of Rome "La Sapienza"
Department of Electrical Engineering
Via Eudossiana, 18 - 00184 Rome (Italy)

(**) University of Rome III
Dept. of Mech. & Indust. Engineering
Via della Vasca Navale, 79 - 00146 Rome (Italy)

Abstract **- The use of a bi-directional dc-dc converter in motor drives devoted to EVs allows a suitable control of both motoring and regenerative braking operations. In particular, during motoring operations of a battery-fed dc motor drive, a dc-dc converter is to be used to adjust the motor current in order to follow the torque reference signal. On the other hand, a bi-directional arrangement of the converter is needed for the reversal of the power flow, in order to recover the vehicle kinetic energy in the battery by means of motor drive regenerative braking operations. This paper deals with the study and comparison of two bi-directional buck-boost converter topologies. Each of them allows stepping the battery voltage level either up or down, according to motor drive modes of operation. For each converter topology computer simulations of modes of operation are presented together with experimental test results.**

I. INTRODUCTION

The use of a bi-directional dc-dc converter in motor drives devoted to the propulsion of EVs allows suitable control of both motoring and regenerative braking operations [1], [2]. This paper deals with the study and comparison of bi-directional buck-boost converter topologies. Each of them allows stepping the battery voltage level either up or down, according to motor drive modes of operation.

The first chosen topology is derived directly from the traditional buck-boost scheme by introducing a dual switch-diode power module as shown in Fig. 1. The IGBTs S_1 and S_2 are never operated at the same time, being the switch S_2 always off during motoring operation, whereas the switch S_1 is kept off continuously whenever the regenerative braking operation is commanded. For the transition from S_1 switching operation to S_2 switching operation a delay blanking time between the gate signals of the two switches is used, in order to avoid a cross-conduction current through the converter output capacitor and the two switches.

The layout of the second topology being considered in this study is accomplished by means of the cascade of a step-down converter with a step-up one, as shown in Fig. 2. In motoring operation, S_1 is switching whenever stepping-down of the battery level is needed, whereas S_2 is operated as a step-up switch while S_1 is permanently in the on state. On the other hand, S_3 and S_4 are modulated in a similar manner but during braking operation.

The converter topology shown in Fig. 2 allows driving in a separate fashion a single switch for each particular condition of operation. In this way, precise regulation of the output voltage can be achieved, as the duty-cycle is allowed to range from 0 to 1 both in step-up and step-down modes of operation. A natural drawback of the buck-boost cascade form is that both switches and power diodes are duplicated with respect to the converter arrangement shown in Fig. 1.

Both the proposed converter topologies require one inductor and two electrolytic capacitors. However, it is shown later on that for a given current ripple the buck-boost cascade topology requires an inductor having reduced size in comparison with the size of the inductor needed in a conventional bi-directional buck-boost topology.

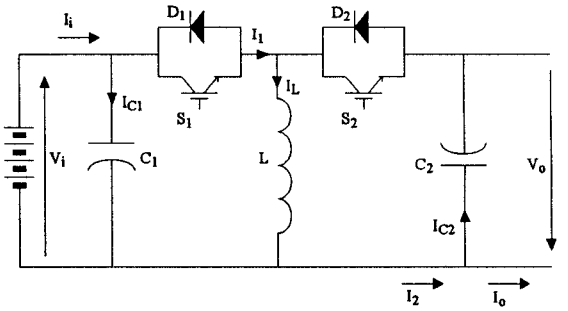

Fig. 1. Bi-directional buck-boost converter

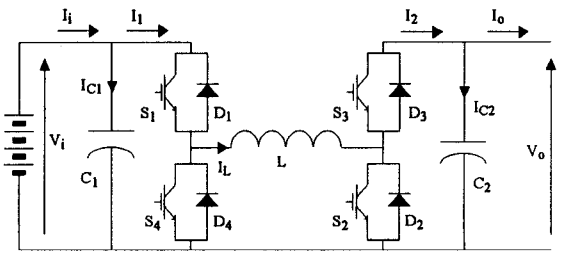

Fig. 2. Bi-directional buck-boost cascade converter

0-7803-4340-9/98/$10.00 © 1998 IEEE.

Each of the proposed converter topologies was early investigated by means of Matlab models to represent modes of operation. However, in order to base comparison on experimental results, two similar 20 kW water-cooled converter prototypes were constructed and tested by using a suitable battery-fed dc motor drive test rig. Each one of the converter prototypes was constructed by using third-generation IGBT power modules rated 1200 V, 200 A, ferrite core inductor rated 420 μH, 80 A, input and output capacitors rated 5600 μF, 450 V. IGBTs switching frequency is 15 kHz and converter control strategy is accomplished by means of an INTEL 80C196KC microcontroller.

II. CONVERTER MODES OF OPERATION

A. Bi-Directional Buck-Boost Converter

In motoring operation the buck-boost converter circuit states are shown in Figg. 3a and 3b respectively when the switch S_1 is on or off. When the switch S_1 is in conduction state, the battery and the output capacitor C_2 supply energy respectively to the inductor L and to the machine load. When the switch S_1 is off, the diode D_2 is direct biased and the output capacitor C_2 and the load receive energy from the inductor. Thereby, the voltage V_0 at the output capacitor terminals can be regulated accordingly with the motor speed by adjusting the duty-cycle of the switch S_1.

Whenever a braking command is issued, the switch S_1 is turned off and, after a fixed blanking time interval, the switch S_2 is turned on to allow the reversal of the power flow. Thereafter, the switch S_2 is operated at constant switching frequency and variable duty-cycle in order to keep at the desired value the braking current flowing in the battery. When the switch S_2 is on, the battery receives energy from the capacitor C_1 while braking energy is being stored in the inductor L. By turning off the switch S_2 the battery and the capacitor C_1 receive energy from the inductor L.

B. Bi-Directional Buck-Boost Cascade Converter

In this converter arrangement only the switch S_1 is operated to accomplish motoring operation with stepping down the battery voltage. The diode D_2 is always reverse biased and D_3 is direct biased along the entire period of operation. As shown in Figg. 4a and 4b, when the switch S_1 is on the battery supplies energy to the inductor L and to the load, whereas with the switch S_1 being in the off state the diode D_4 is direct biased and the load receives energy from the inductor.

In motoring operation the step-up mode of operation is needed at the higher motor speeds. The switch S_1 must be always on and S_2 is operated with variable duty cycle according to motor speed. The switches S_3 and S_4 are steadily off and the diode D_4 is reverse biased.

Circuit states of the cascade converter in motoring step-up conduction mode are shown in Figg. 5a and 5b respectively when the S_2 is on or off. When the switch S_2 is on, the battery supplies energy to the inductor while the load receives energy from the capacitor C_2. As the switch S_2 is off, the diode D_3 is direct biased and load and output capacitor receive energy from the inductor.

Whenever a braking command is issued, the switch S_3 is turned on just after a fixed blanking time interval to allow the reversal of the power flow. Thereafter two condition of braking operation can occur depending on the instantaneous voltage levels of both the battery and the dc motor e.m.f. If the motor e.m.f. is greater than the battery voltage, the converter operates as a step-down converter. Hence, the switch S_3 is operated at constant switching frequency and variable duty-cycle, while S_1, S_2 and S_4 are permanently off. The diode D_4 is always reverse biased and D_1 is direct biased along the entire switching period. As the e.m.f. value goes below the battery voltage, the converter operates in step-up condition. Then, the switch S_3 is always on and the switch S_4 is operated with variable duty cycle; the switches S_1 and S_2 are steadily off.

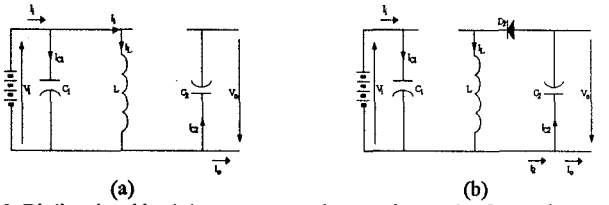

(a) (b)

Fig. 3. Bi-directional buck-boost converter in motoring mode of operation: (a) switch on, (b) switch off

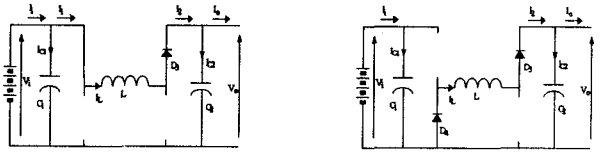

(a) (b)

Fig. 4. Bi-directional buck-boost cascade converter in motoring step-down mode of operation: (a) switch on, (b) switch off

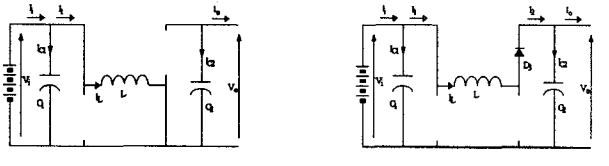

(a) (b)

Fig. 5. Bi-directional buck-boost cascade converter in motoring step-up mode of operation: (a) switch on, (b) switch off

III. COMPARISON BETWEEN THE PROPOSED TOPOLOGIES

In order to develop a comparison between the above discussed converter topologies, theoretical expressions of the currents flowing through the converter components were worked out. Plots of duty cycle, current ripple and rms value as function of the ratio V_o/V_i between the converter output and input voltages are shown in Fig. 6 through Fig. 12. These plots refer to converter operation assuming as reference input voltage V_i = 180V, reference output current I_o =35A, switching frequency f_s =15kHz and are based on the use of an inductor having L = 420μH.

If the duty cycle of the switch in the buck-boost converter is indicated as D_b, and D_{cd} and D_{cu} are the duty cycles of the working switch in the buck-boost cascade topology respectively during step-down and step-up mode of operation, the output voltage Vo can be calculated as:

$$V_o = \frac{D_b}{1-D_b}\cdot V_i \qquad 0 < D_b < 1 \qquad (1)$$

$$V_o = \frac{D_{cd}}{1-D_{cu}}\cdot V_i \quad \begin{cases} 0 < D_{cd} < 1 \ \& \ D_{cu} = 1 \\ D_{cd} = 1 \ \& \ 0 < D_{cu} < 1 \end{cases} \qquad (2)$$

Consequently, the duty cycle expressions as function of voltage ratio V_o/V_i are:

$$D_b = \frac{V_o/V_i}{1+V_o/V_i} \qquad 0 < D_b < 1 \qquad (3)$$

$$D_{cd} = \frac{V_o}{V_i}\left(1-D_{cu}\right) \qquad D_{cu} = 0;\ V_o < V_i \qquad (4)$$

$$D_{cu} = 1-\frac{D_{cd}}{V_o/V_i} \qquad D_{cd} = 1;\ V_o > V_i \qquad (5)$$

Fig. 6 shows that in the step-down mode of operation the duty cycle D_b of buck-boost topology is always lower than the duty cycle D_{cd} value required in buck-boost cascade topology. On the other hand, the D_b is always greater than D_{cu} in step-up conduction mode. This fact results in greater current ripple and rms value in a number of converter components as shown later on.

Full theoretical expressions of inductor current ripple, inductor, capacitors and power semiconductor components rms current are presented in the Appendix. Fig. 7 shows that the ripple of inductor current in p.u. respect to the output current is greater in buck-boost converter than in buck-boost cascade one. This difference is particularly remarkable when the output voltage level is close to the battery voltage value. Also, for a given value of the ratio V_o/V_i, the rms value of the inductor current is higher in bi-directional buck-boost topology.

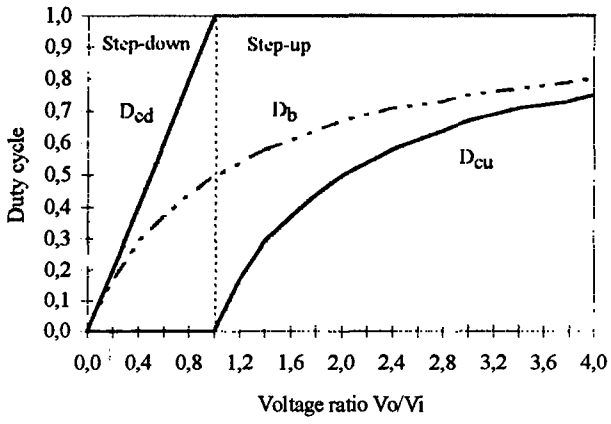

Fig. 6. Duty cycle versus V_o/V_i of buck-boost (dashed trace) and of buck-boost cascade (line trace)

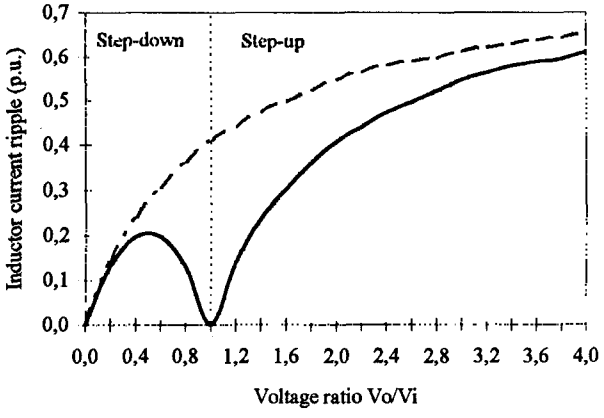

Fig. 7. Inductor current ripple versus V_o/V_i in buck-boost (dashed trace) and buck-boost cascade (line trace)

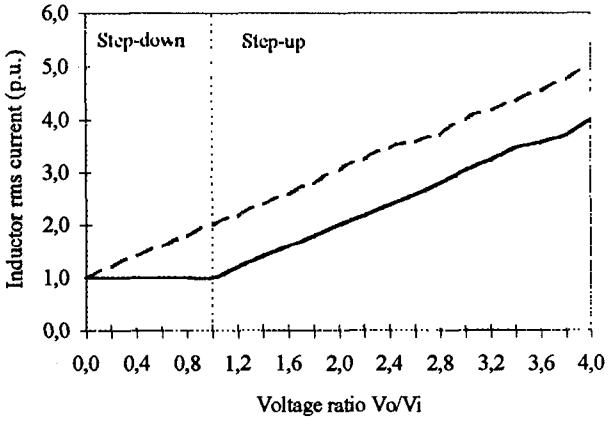

Fig. 8. Inductor rms current versus V_o/V_i in buck-boost (dashed trace) and buck-boost cascade (line trace)

Fig. 8 shows the p.u. value of inductor rms current (I_L) as a function of the voltage ratio.

During step-down mode of operation, the inductor rms current of buck-boost cascade converter is nearly constant and equal to the output current value, as in any instant the inductor current is the output current too. On the contrary, in the step-up mode of operation the modulating switch being in the on state, the load is fed by the output capacitor C_2 and the inductor L is connected in parallel to the input source. This results in inductor rms current which increases accordingly with the ratio V_o/V_i.

Concerning voltage ratios greater than 1, the buck-boost inductor current exceeds the buck-boost cascade inductor current of a quantity equal to the output current.

Hence, the inductor in the buck-boost configuration operates under higher electric and thermal stress, turning out in greater power losses and saturation of the ferrite core reached for a lower value of the voltage ratio V_o/V_i

Figg. 9 and 10 show the current rms value respectively in the input and output capacitor C_1 (I_{C1}) and C_2 (I_{C2}) of both the converter topologies being under investigation. The curves shown in Fig. 9 reveal that the input capacitor works in a similar manner in both the converters, and the rms current is always below the output current I_o along the entire ratio V_o/V_i range. On the other hand, the output capacitor is more stressed in buck-boost than in buck-boost cascade topology. As shown in Fig. 10, the output capacitor rms current is higher in the first configuration than in the second one of an average amount equal to the 1/3 of the output current. Besides at high values of the voltage ratio the output capacitor current results twice the output current I_o.

Figg. 11 and 12 show the rms current diagrams of the switch and the diode in switching mode of operation. It is again found that the buck-boost topology results in higher current stress on both switch and diode compared to buck-boost cascade. In detail, during step-up mode of operation, the switch rms current in the buck-boost configuration results nearly equal to the current in the second one added up I_o. Thus turning out in higher switching and conduction power losses in buck-boost converter.

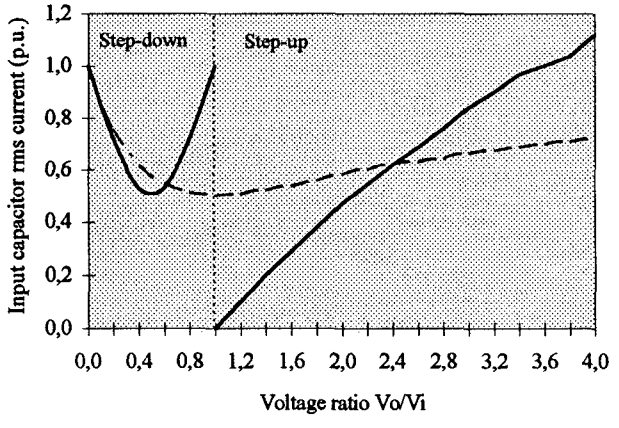

Fig. 9. Current ripple rms value of C_1 versus V_o/V_i in buck-boost (dashed trace) and buck-boost cascade (line trace)

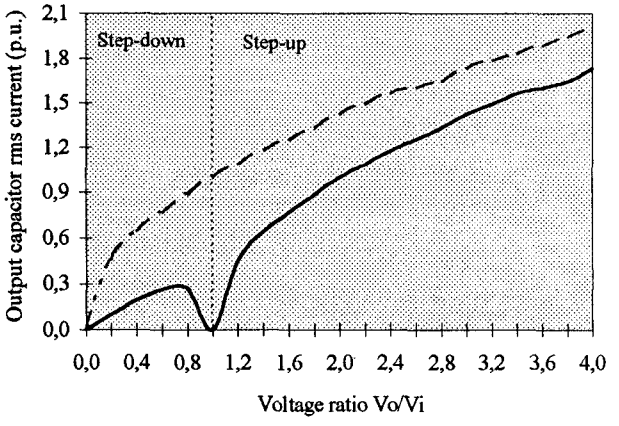

Fig. 10. Current ripple rms value of C_2 versus V_o/V_i in buck-boost (dashed trace) and buck-boost cascade (line trace)

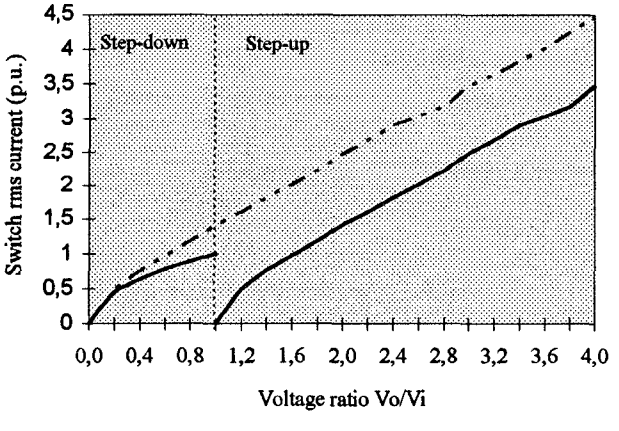

Fig. 11. Switch rms current versus V_o/V_i in buck-boost (dashed trace) and buck-boost cascade (line trace)

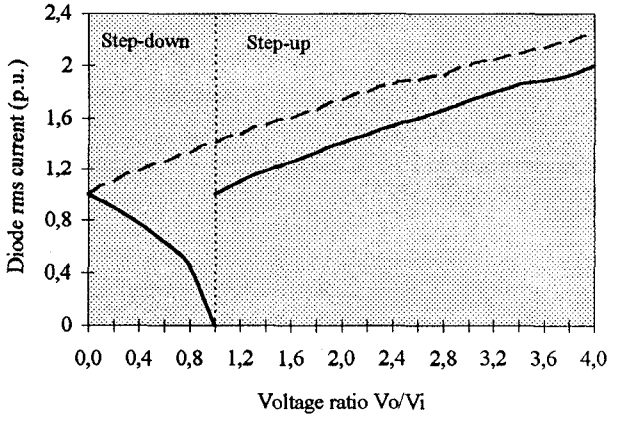

Fig. 12. Diode rms current versus V_o/V_i in buck-boost (dashed trace) and buck-boost cascade (line trace)

The carried out analysis confirm that higher electric and thermal stress, as well as a lower converter efficiency characterize the mode of operation of the bi-directional buck-boost configuration with respect to the bi-directional buck-boost cascade one.

IV. SIMULATION AND EXPERIMENTAL RESULTS

Concerning the two converter topologies being under investigation, computer analysis was performed by using Matlab models which describe the converter modes of operation. In addition, a test campaign was carried out by using a motor drive arrangement as shown in Fig. 13.

Fig. 14 shows the Matlab model of dc motor drive, arranged with a buck-boost cascade converter.

Waveforms of the output current I_o, inductor current I_L and output capacitor current I_{C2} in both step-down and step-up mode of operation are plotted in Figg. 15 and 16 for the bi-directional buck-boost converter and in Figg. 17 and 18 for the bi-directional buck-boost cascade converter. According to theoretical considerations, simulation results put into evidence that the buck-boost converter is more stressed than the cascade one. As a result, it needs a greater sizing of converter components to gain the same features in a given working condition.

Figg. 19, 20, 21 and 22 show waveforms achieved from experimental test campaign. Comparing experimental curves with simulation results shown in Fig. 15 through Fig. 18 it can be remarked the similarity of the waveforms and then the validation of both theoretical study and simulation models.

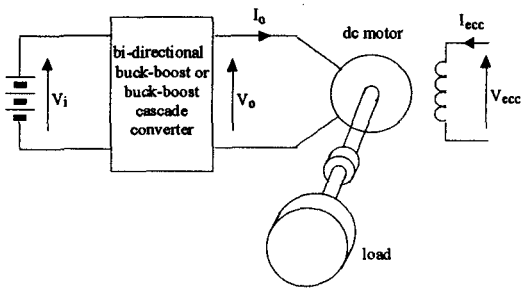

Fig. 13. Layout of the drive arrangement

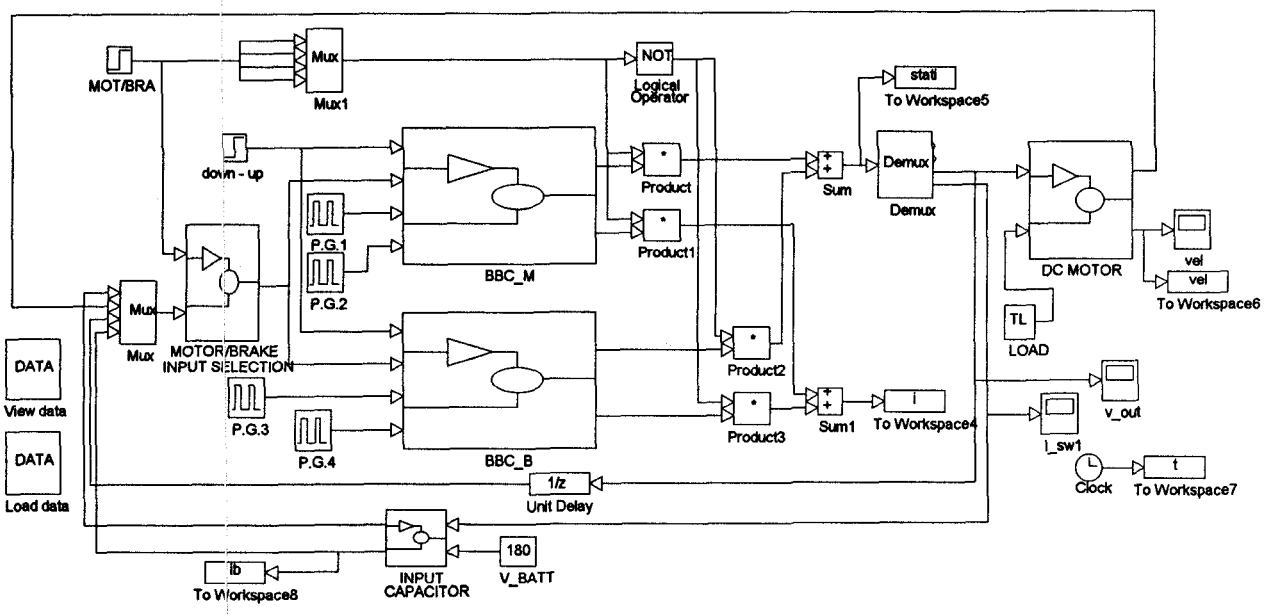

Fig. 14. Matlab model of dc motor drive with buck-boost cascade converter

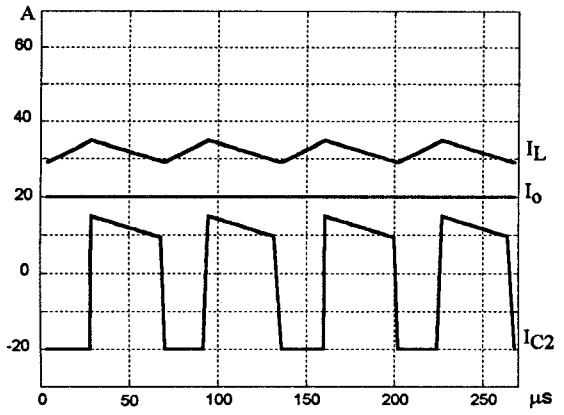

Fig. 15. Simulation results: inductor (I_L), output capacitor (I_{C2}) and output (I_o) currents in buck-boost converter in step-down mode of operation (current scale 10A/div, time scale 50μs/div)

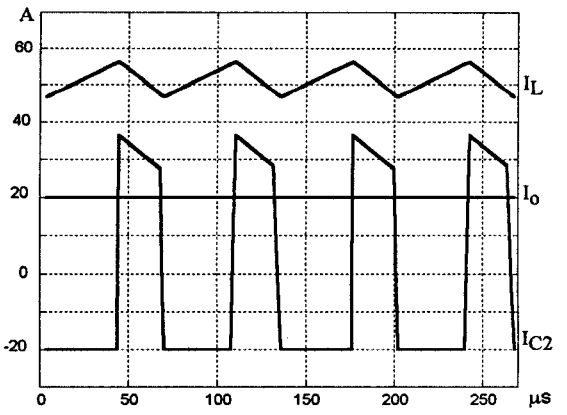

Fig. 16. Simulation results: inductor (I_L), output capacitor (I_{C2}) and output (I_o) currents in buck-boost converter in step-up mode of operation (current scale 10A/div, time scale 50μs/div)

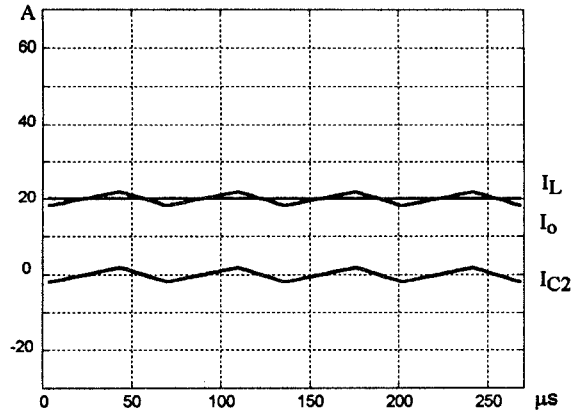

Fig. 17. Simulation results: inductor (I_L), output capacitor (I_{C2}) and output (I_o) currents in buck-boost cascade converter in step-down mode of operation (current scale 10A/div, time scale 50μs/div)

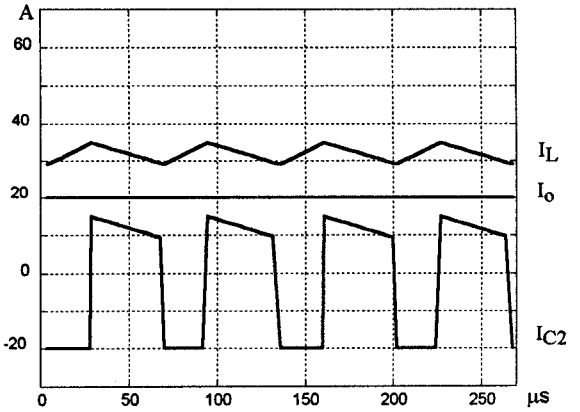

Fig. 18. Simulation results: inductor (I_L), output capacitor (I_{C2}) and output (I_o) currents in buck-boost cascade converter in step-up mode of operation (current scale 10A/div, time scale 50μs/div)

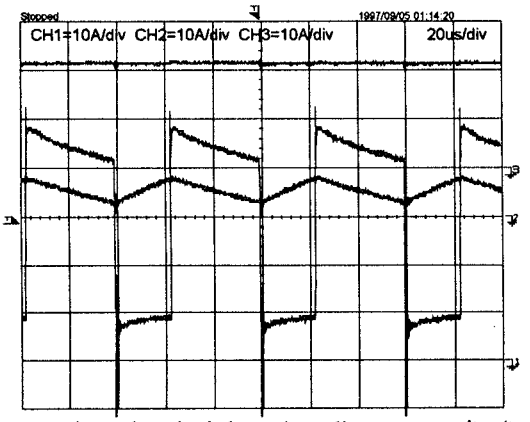

Fig. 19. Experimental results: inductor (trace 1), output capacitor (trace 2) and output (trace 3) currents in buck-boost converter in step-down mode of operation (current scale 10A/div, time scale 20μs/div)

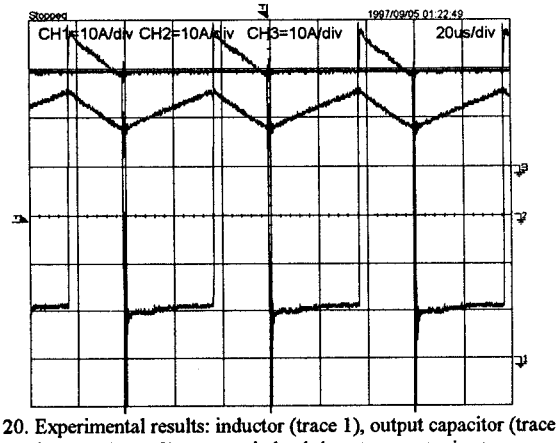

Fig. 20. Experimental results: inductor (trace 1), output capacitor (trace 2) and output (trace 3) currents in buck-boost converter in step-up mode of operation (current scale 10A/div, time scale 20μs/div)

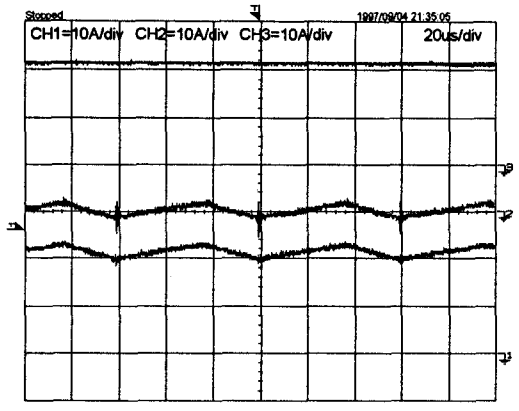

Fig. 21. Experimental results: inductor (trace 1), output capacitor (trace 2) and output (trace 3) currents in buck-boost cascade converter in step-down mode of operation (current scale 10A/div, time scale 20µs/div)

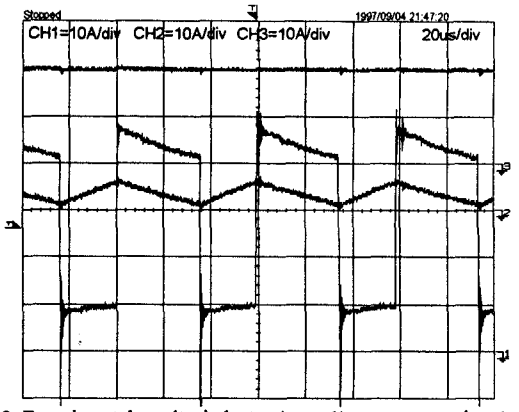

Fig. 22. Experimental results: inductor (trace 1), output capacitor (trace 2) and output (trace 3) currents in buck-boost cascade converter in step-up mode of operation (current scale 10A/div, time scale 20µs/div)

V. CONCLUSIONS

This paper has discussed the comparison between bi-directional buck-boost converter topology and bi-directional buck-boost cascade converter topology. Simulation and preliminary experimental results were achieved by using Matlab models and by carrying out a campaign test on 20 kW water-cooled converter prototypes.

The comparison results point out that higher electric and thermal stress characterize the operation of the bi-directional buck-boost configuration with respect to the bi-directional buck-boost cascade one. In step-down mode of operation the two topologies differences are not very large, whilst in step-up mode of operation the current rms value of inductor, power switches and output capacitor, is greater of an amount, respectively equal to the output current I_o and to 1/3 of the output current I_o, in buck-boost converter with respect to buck-boost cascade converter. In conclusion, even if in the buck-boost cascade topology both switches and power diodes are duplicated with respect to the buck-boost one, reduced size inductor and capacitors can be used, thus gaining back the cost increment due to the power semiconductor components.

REFERENCES

[1] Caricchi, F. Crescimbini, G. Noia, D. Pirolo, "Experimental study of a bidirectional dc-dc converter for the dc link voltage control and regenerative braking in PM motor drives devoted to electrical vehicles," *Proceedings of the IEEE 9th Applied Power Electronics Conference and Exposition (APEC'94)*, Orlando, Florida (USA), February 13-17, 1994.

[2] Caricchi, F. Crescimbini, A. Di Napoli, M. Marcheggiani, "Prototype of electric vehicle drive with twin water-cooled wheel direct drive motors," *Proceedings of the 27th Annual IEEE Power Electronics Specialists Conference (PESC'96)*, Baveno (Italy), June 23-27, 1996.

APPENDIX

Assuming f_s as the switching frequency, V_i the input voltage, I_o the output current and L the inductance value, inductor current ripple (ΔI_L), inductor (I_L), input and output capacitor (I_{C1}, I_{C2}), power switch (I_S), and diode (I_D) rms current can be calculated as:

1) Buck-Boost Converter

$$\Delta I_{L,b} = \frac{V_i \cdot D_b}{f_s \cdot L} \tag{6}$$

$$I_{L,b} = \sqrt{\left(\frac{I_o}{1-D_b}\right)^2 + \frac{1}{3}\cdot\left(\frac{\Delta I_{L,b}}{2}\right)^2} \tag{7}$$

$$I_{C1,b} = I_o \cdot \sqrt{1-3\cdot D_b \cdot (1-D_b)} \tag{8}$$

$$I_{C2,b} = I_o \cdot \sqrt{\frac{D_b}{1-D_b}} \tag{9}$$

$$I_{S,b} = I_{L,b} \cdot \sqrt{D_b} \tag{10}$$

$$I_{D,b} = I_{L,b} \cdot \sqrt{(1-D_b)} \tag{11}$$

2) Buck-Boost Cascade Converter in Step-Down Mode of Operation

$$\Delta I_{L,cd} = \frac{V_i \cdot D_{cd}}{f_s \cdot L}\cdot(1-D_{cd}) \tag{12}$$

$$I_{L,cd} = \sqrt{I_o^2 + \frac{1}{3}\cdot\left(\frac{\Delta I_{L,cd}}{2}\right)^2} \tag{13}$$

$$I_{C1,cd} = I_o \cdot \sqrt{1-3\cdot D_{cd}\cdot(1-D_{cd})} \tag{14}$$

$$I_{C2,cd} = \Delta I_{L,cd} \cdot \sqrt{\frac{2\cdot D_{cd}+1}{3\cdot(1-D_{cu})}} \tag{15}$$

$$I_{S,cd} = I_{L,cd} \cdot \sqrt{D_{cd}} \tag{16}$$

$$I_{D,cd} = I_{L,cd} \cdot \sqrt{(1-D_{cd})} \tag{17}$$

3) Buck-Boost Cascade Converter in Step-Up Mode of Operation

$$\Delta I_{L,cu} = \frac{V_i \cdot D_{cu}}{f_s \cdot L} \tag{18}$$

$$I_{L,cu} = \sqrt{\left(\frac{I_o}{1-D_{cu}}\right)^2 + \frac{1}{3}\cdot\left(\frac{\Delta I_{L,cu}}{2}\right)^2} \tag{19}$$

$$I_{C1,cu} = \Delta I_{L,cu} \cdot \sqrt{\frac{2\cdot D_{cu}+1}{3\cdot(1-D_{cu})}} \tag{20}$$

$$I_{C2,cu} = I_o \cdot \sqrt{\frac{D_{cu}}{1-D_{cu}}} \tag{21}$$

$$I_{S,cu} = I_{L,cu} \cdot \sqrt{D_{cu}} \tag{22}$$

$$I_{D,cu} = I_{L,cu} \cdot \sqrt{(1-D_{cu})} \tag{23}$$